European Journal of Pharmacology 966 (2024) 176329

Contents lists available at ScienceDirect

European Journal of Pharmacology

journal homepage: www.elsevier.com/locate/ejphar

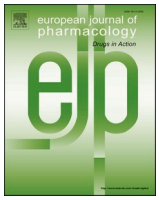

The novel non-hallucinogenic compound DM506 (3-methyl-1,2,3,4,5,6-hexahydroazepino[4,5-*b*]indole) induces sedative- and anxiolytic-like activity in mice by a mechanism involving 5-HT_{2A} receptor activation

Hugo R. Arias [a], Deborah Rudin [b,c], Dustin J. Hines [d], April Contreras [d], Alican Gulsevin [e,f], Dina Manetti [g], Youssef Anouar [k], Philippe De Deurwaerdere [h], Jens Meiler [i], Maria Novella Romanelli [g], Matthias E. Liechti [b,c], Abdeslam Chagraoui [j,k,*]

[a] *Department of Pharmacology and Physiology, Oklahoma State University College of Osteopathic Medicine, Tahlequah, OK, USA*
[b] *Divison of Clinical Pharmacology and Toxicology, Department of Pharmaceutical Sciences, University of Basel, Basel, Switzerland*
[c] *Division of Clinical Pharmacology and Toxicology, Department of Biomedicine, University Hospital Basel and University of Basel, Basel, Switzerland*
[d] *Psychological and Brain Sciences, University of Nevada, Las Vegas, NV, USA*
[e] *Department of Chemistry, Vanderbilt University, Nashville, TN, USA*
[f] *Center for Structural Biology, Vanderbilt University, Nashville, TN, USA*
[g] *Department of Neurosciences, Psychology, Drug Research and Child Health Section of Pharmaceutical and Nutraceutical Sciences, University of Florence, Italy*
[h] *Centre National de la Recherche Scientifique, Institut des Neurosciences Integratives et Cognitives d'Aquitaine, UMR, 5287, Bordeaux, France*
[i] *Institute for Drug Discovery, Leipzig University Medical School, 04103, Leipzig, Germany*
[j] *Department of Medical Biochemistry, Rouen University Hospital, CHU de Rouen, France*
[k] *UNIROUEN, Inserm U1239, Neuroendocrine, Endocrine and Germinal Differentiation and Communication (NorDiC), Rouen Normandie University, 76000, Mont-Saint-Aignan, France*

ARTICLE INFO

Keywords:
Ibogaminalog
Anxiolytic activity
Sedative activity
5-$HT_{2A/2B}$ receptors
Molecular docking

ABSTRACT

The anxiolytic and sedative-like effects of 3-methyl-1,2,3,4,5,6-hexahydroazepino[4,5-b]indole (DM506), a non-hallucinogenic compound derived from ibogamine, were studied in mice. The behavioral effects were examined using Elevated O-maze and novelty suppressed feeding (NSFT) tests, open field test, and loss of righting reflex (LORR) test. The results showed that 15 mg/kg DM506 induced acute and long-lasting anxiolytic-like activity in naive and stressed/anxious mice, respectively. Repeated administration of 5 mg/kg DM506 did not cause cumulative anxiolytic activity or any side effects. Higher doses of DM506 (40 mg/kg) induced sedative-like activity, which was inhibited by a selective 5-HT_{2A} receptor antagonist, volinanserin. Electroencephalography results showed that 15 mg/kg DM506 fumarate increased the transition from a highly alert state (fast γ wavelength) to a more synchronized deep-sleeping activity (δ wavelength), which is reflected in the sedative/anxiolytic activity in mice but without the head-twitch response observed in hallucinogens. The functional, radioligand binding, and molecular docking results showed that DM506 binds to the agonist sites of human 5-HT_{2A} (Ki = 24 nM) and 5-HT_{2B} (Ki = 16 nM) receptors and activates them with a potency (EC_{50}) of 9 nM and 3 nM, respectively. DM506 was relatively less potent and behaved as a partial agonist (efficacy <80%) for both receptor subtypes compared to the full agonist DOI (2,5-dimethoxy-4-iodoamphetamine). Our study showed for the first time that the non-hallucinogenic compound DM506 induces anxiolytic- and sedative-like activities in naïve and stressed/anxious mice in a dose-, time-, and volinanserin-sensitive manner, likely through mechanisms involving 5-HT_{2A} receptor activation.

* Corresponding author. Department of Physiology and Biochemistry, CHU de Rouen, France. UNIROUEN, Inserm U1239, Neuroendocrine, Endocrine and Germinal Differentiation and Communication (NorDiC), Rouen Normandie University, 76000, Mont-Saint-Aignan, France.
E-mail address: abdeslam.chagraoui@univ-rouen.fr (A. Chagraoui).

https://doi.org/10.1016/j.ejphar.2024.176329
Received 30 October 2023; Received in revised form 9 January 2024; Accepted 10 January 2024
Available online 20 January 2024

1. Introduction

Preclinical research on mood disorders is actively producing medications for mood disorders that could circumvent the main issues with selective serotonin reuptake inhibitors. These issues include treatment resistance in a substantial number of patients, delayed onset of efficacy, and specific side effects. (Bose et al., 2012; Hicks et al., 2015; Vahid-Ansari et al., 2019). Clinical data suggest that drugs such as psychedelics may overcome the resistance to current antidepressant/anxiolytic medications and provide a short onset of action (Cameron et al., 2023; Carhart-Harris et al., 2021; Dos Santos et al., 2021; Holze et al., 2020, 2023; Pedzich et al., 2022). Although these compounds may be considered for novel therapeutic uses, they require specific conditions, owing to their ability to induce acute hallucinogenic effects and anxiety. Therefore, the development of psychoplastogens for safer therapeutic treatment of various neuropsychiatric conditions is needed.

Classic psychedelics exhibit a complex pharmacological profile that converges towards serotonergic receptors, particularly 5-HT_{2A} receptors. Various classic psychedelics, including mescaline, psilocybin, N,N-dimethyltryptamine, lysergic acid diethylamide (LSD), TCB-2 [(4-bromo-3,6-dimethoxybenzocyclobuten-1-yl)methylamine], and DOI [(±)-2,5-dimethoxy-4-iodoamphetamine], bind 5-HT_{2A} receptors and/or modify their function. The 5-HT_{2A} receptor is highly expressed in the brain, particularly in the cortex (Weber and Andrade, 2010). Visual hallucinations caused by serotonergic hallucinogens, such as psilocybin and LSD, are primarily mediated through 5-HT_{2A} receptors (Nichols, 2004; Vollenweider and Kometer, 2010). However, other 5-HT2A receptor agonists such as lisuride do not induce psychedelic effects in humans (Liu et al., 2022) and do not promote head twitching responses in mice, a simple behavioural model to address the hallucinogenic properties of drugs in humans (Halberstadt, 2015). The mechanisms behind the non-psychedelic properties of some 5-HT2A receptor agonists could lie in their biased agonism profile (Cao et al., 2022b; Diez-Alarcia et al., 2021; Gonzalez-Maeso et al., 2007; Muguruza et al., 2014; Muneta-Arrate et al., 2020) and/or their action on other targets.

Novel compounds derived from iboga alkaloids (ibogalogs), such as tabernanthalog (TBG), induce antiaddictive, antidepressant, and anxiolytic-like activities (Cameron et al., 2021; Heinsbroek et al., 2023; Lu et al., 2021). DM506 (Fig. 1) is a recently synthesized derivative of ibogamine (Cameron et al., 2021; Tae et al., 2023), a member of the iboga family comprising alkaloids that exhibit the above-mentioned properties (Arias et al., 2020b, 2023a, 2023b; Luz and Mash, 2021; Rodriguez et al., 2020). It has a complex pharmacological profile, including cholinergic actions, but its ability to trigger 5-HT_{2A} receptor-dependent responses has not been explored notably in anxiolytic responses.

In this study, we investigated the anxiolytic- and sedative-like activities of DM506 (3-methyl-1,2,3,4,5,6-hexahydroazepino[4,5-*b*]indole) in mice. The anxiolytic-like activity of DM506 was determined in naïve and stressed/anxious mice using the elevated O-maze and novelty-suppressed feeding tests (NSFT), whereas its sedative activity was determined using the open field and loss of righting reflex (LORR) tests (Arias et al., 2023b). The head-twitch response test was used to assess whether DM506 has hallucinogenic properties (Fox et al., 2010). The involvement of 5-HT_{2A} and/or 5-HT_{2B} receptors in the anxiolytic-like activity of DM506 was investigated using volinanserin, a selective 5-HT_{2A} receptor antagonist (Casey et al., 2022; Jaster et al., 2022). In addition, the binding affinity, functional activity, and molecular docking of DM506 at both 5-HT_{2A} and 5-HT_{2B} receptors was determined, and electroencephalographic (EEG) activity was assessed in freely moving mice.

Abbreviations

5-HT	5-hydroxytryptamine (serotonin)
DM506 (ibogaminalog)	3-methyl-1,2,3,4,5,6-hexahydroazepino [4,5-*b*]indole
TBG (tabernanthalog)	8-methoxy-3-methyl-1,2,3,4,5,6-hexahydroazepino[4,5-b]indole fumarate
DOI	2,5-dimethoxy-4-iodoamphetamine
TCB-2	(4-bromo-3,6-dimethoxybenzocyclobuten-1-yl) methylamine
volinanserin (MDL 100907)	(R)-(+)-α-(2,3-dimethoxyphenyl)-1-[2-(4-fluorophenyl)ethyl]-4-pipidinemethanol
LSD	lysergic acid diethylamide
NSFT	novelty-suppressed feeding test
LORR	loss of righting reflex
RT	room temperature
EEG	electroencephalography
FFT	fast Fourier transform
P1/P2	phase 1 and 2
IC_{50}	ligand concentration that produces 50% binding inhibition
EC_{50}	ligand concentration that produces 50% response
K_i	inhibitory constant
IP1	inositol monophosphate 1
MD	molecular dynamics
RMSD	root mean square deviation

2. Materials and methods

2.1. Materials

[^{3}H]LSD (82.8 Ci/mmol) was obtained from PerkinElmer (Schwerzenbach, Switzerland). DOI (2,5-dimethoxy-4-iodoamphetamine) was obtained from Lipomed AG (Arlesheim, Switzerland). 5-HT hydrochloride (serotonin) was purchased from Merck (Buchs, Switzerland). Volinanserin (also known as MDL100907 or M100907) [(R)-(+)-α-(2,3-dimethoxyphenyl)-1-[2-(4-fluorophenyl)ethyl]-4-pipidinemethanol] was purchased from AdooQ BioScience (CA, USA). TCB-2 [(4-bromo-3,6-dimethoxybenzocyclobuten-1-yl)methylamine hydrobromide] and DOI [(±)-2,5-dimethoxy-4-iodoamphetamine hydrochloride] were purchased from Biotechne-Tocris (Rennes, France). Dimethyl sulfoxide (DMSO) was purchased from Sigma-Aldrich (Saint Quentin Fallavier, France). Isoflurane was supplied by Covetrus, North America (Dublin, Ohio, USA). DM506 (base and fumarate salts) was synthesized as previously described (Tae et al., 2023). Salts, solvents, and reagents were obtained from commercial suppliers.

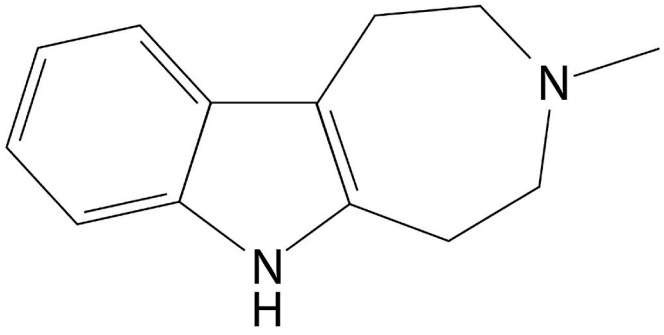

Fig. 1. Molecular structure of DM506 (3-methyl-1,2,3,4,5,6-hexahydroazepino [4,5-*b*]indole) in stick representation. Considering a pK_a value of −1.82 for DM506 (calculated using the Biovia Discovery Studio software (Dassault Systèmes Co., MA, USA), the azepino N-methyl group is 100% protonated at physiological pH.

2.2. Behavioral experiments

2.2.1. Animals

All experimental procedures were performed in accordance with the National Institute of Health Guide for the Care and Use of Laboratory Animals, approved by the Regional Ethics Committee for Animal Experimentation, and carried out in accordance with the European Communities Council Directive (86/609/EEC + 2010/63/UE) and the Institutional Animal Care Committee (animal experimentation ethics committee n°054, 2023, France).

Adult male (30–35 g) Swiss albino CD1 (Electroencephalography recording) and C57BL/6J (for behavioral tests) mice were purchased from Janvier Labs (Le Genest Saint Isle, France) and Jackson Laboratory (Sacramento, CA, USA), respectively. The animals were housed in groups with free access to standard diet and water. The animals were kept in a ventilated room at a temperature of 22 ± 1 °C under a 12 light/12-h dark cycle.

2.2.2. Open field test

To determine whether DM506 induced locomotor activity, open-field experiments were performed, as previously described (Arias et al., 2023b). Mice (n = 10/condition) were habituated to the experimental room 24 h before the experiments. The following day, each mouse was injected (i.p.) with a single dose (15 or 40 mg/kg) of DM506 (base) [dissolved in vehicle: DMSO (1%) and NaCl (0.9%)], and locomotor activity was assessed 15 min after the last injection.

The animals were placed in a 20 × 20 × 30 cm compartment, in a dimly illuminated and quiet room. Mice locomotor activity was automatically monitored using a computerized actimeter (Versamax; AccuScan Instruments, Inc., OH, USA). Horizontal movements determined by the number of crossed beams were recorded every 10 min for a total duration of 60 min.

2.2.3. Elevated O-maze test

The anxiolytic-like activity of DM506 was evaluated in naïve mice using the elevated O-maze test, as previously described (Arias et al., 2023b). Mice (n = 10/condition) were habituated to the experimental room 24 h prior to the experiments. The following day, mice were injected (i.p.) with a single dose (5 or 15 mg/kg) of DM506 (base) [dissolved in vehicle: DMSO (1%), NaCl (0.9%)], or vehicle. The anxiolytic-like activity of the compound was determined after 1 and 24 h (acute effect), and after 48, 72, and 96 h (long-lasting effect). The involvement of the 5-HT_{2A} receptor was assessed by administering 0.05 mg/kg volinanserin (s.c.), an antagonist with high selectivity for the 5-HT_{2A} receptor (Casey et al., 2022; Jaster et al., 2022), 15 min before DM506. To assess whether the efficacy of the compound increased after repeated treatment, mice were injected with 5 mg/kg DM506 (i.p.) for 10 consecutive days, and the elevated O-maze test was performed on day 5 and day 10, respectively, 15 min after the last injection.

The elevated O-maze session began by gently placing the mouse, with its nose facing one of the closed arms of the maze, allowing it to explore freely. The sessions were recorded for 5 min using an automated image analysis system (Ethovision XT v13.0; Noldus Information Technologies, Wageningen, Netherlands) placed at the top of the maze. The position of the mouse in each area (open or closed arms) was determined by the center of gravity of its image (recorded by a camera placed approximately 2 m at about 2 m above the maze). The relative degree of fear or anxiety can be assessed by comparing the time spent in the closed arms with the time spent in the open arms, and the number of entries into the closed arms. The maze was cleaned with a 20% ethanol solution and dried with a cloth between sessions.

2.2.4. Novelty-suppressed feeding test

To assess the anxiolytic-like activity of DM506 in mice under stressful/anxiogenic conditions, the novelty-suppressed feeding test (NSFT) was performed as previously described (Arias et al., 2020a, 2023b). Mice (n = 10/condition) were deprived of food for 24 h. The following day, the animals were injected (i.p.) with 15 mg/kg DM506 (base) or vehicle. To determine whether 5-HT_{2A} receptors are involved in the effects of DM506, mice were injected (s.c.) with 0.05 mg/kg volinanserin 15 min before DM506. One and 24 h after the last injection, the following parameters were measured (see Fig. 4A), as previously described (Arias et al., 2023a): latency to approach the center of the field, latency to eat, food consumption during the first 10 min after NSFT, and in-cage latency to eat.

The apparatus consisted of a highly illuminated open field (40 cm × 60 cm). A small pellet of the usual food was placed on a platform consisting of a Petri dish with a white circle cut from Whatman paper using the side walls of the Petri dish as a base to stabilize the position in the bedding (see Fig. 3A). On the day of testing, each mouse was gently and randomly placed in a corner of the arena, and the timer was started immediately. The animals first approached the food pellet, sniffed it without biting it, and then grasped it with their front paws and bit it. The latency to approach the center and/or eat food was recorded for 5 min.

2.2.5. Loss of righting reflex (LORR) test

To determine the sedative/hypnotic effects of DM506, LORR tests were performed, as previously described (Arias et al., 2023b). Mice (n = 10/condition) were acclimated to the experimental room for 24 h before the experiments. The following day, mice were injected (i.p.) with 15 mg/kg or 40 mg/kg DM506 (base) or vehicle. To determine the involvement of the 5-HT_{2A} receptor in the sedative activity of 40 mg/kg DM506, volinanserin (0.05 mg/kg; s.c.) was injected 15 min before DM506.

Thirty minutes after drug injection, when the mice became motionless, they were individually placed on their backs in a dorsal recumbent position in a V-shaped plexiglass until they were able to back up right themselves within 10 min. The experimenter observed the mice until they turned all four paws over and stood upright. Immobility time was defined as the time from placement in the supine position until the animals regained their righting reflex.

2.2.6. Head-twitch response test

After 15 min of acclimatization in a Plexiglas container, mice (n = 10/condition) were administered DM506 (10, 15, 25, or 40 mg/kg; i.p.) or vehicle, and the head-twitch response was compared to that induced by TCB-2 (1 mg/kg, i.p.) and DOI (1 mg/kg, i.p.) (dissolved in water), two agents that induce a head-twitch response (Halberstadt, 2015). Five minutes after drug administration, head-twitch responses were recorded once every 5 min at five 1 min intervals for 30 min on mice located inside bedding-lined transparent plastic cages. The cumulative values of the five 1 min intervals were summed (Fox et al., 2010).

2.2.7. Electroencephalography recording

Electroencephalography (EEG) electrodes were implanted in each mouse under isoflurane anesthesia (4% induction, and maintained at 0.5–1%, in 2 L/min oxygen). Two EEG channels were recorded bilaterally from the frontal cortex, with placement in the caudal parietal area to provide a baseline. After a minimum of seven days of postoperative recovery, mouse EEG activity was recorded at a sampling rate of 1000 Hz using the Pinnacle 8400 series system (Pinnacle Technology, Inc., Lawrence, Kansas, USA) during the dark phase of the cycle. The mice were acclimatized to the recording chamber and pinnacle preamplifier for 1 h. EEG recordings were obtained from eight mice prior to DM506 administration to provide baseline reference data as controls. During baseline recordings, sleep was suppressed or interrupted by the introduction of novel objects when the animals showed behavioral and EEG indications of sleep. After 1 h of baseline recording, the mice were administered (i.p.) 15 mg/kg DM506 fumarate (corresponding to 11.6 mg/kg DM506 base), and EEG was recorded for another hour. The results were quantified using SleepSign (KISSEI COMTEC, Nagano, Japan) and Python (https://www.python.org/). Fast Fourier transform (FFT)

was used to parse the data into spectral frequency divisions according to the following limits (Hines et al., 2018, 2022): δ (0.4–4.0 Hz), found in slow wave or non-rapid eye movement (NREM) sleep, θ (4.0–8.0 Hz), observed during rapid eye movement (REM) sleep, α (8.0–13.0 Hz), observed during relaxed, awake, calm, or meditative states, β (13.0–30.0), associated with active, alert, and focused states, and γ (30.0–100 Hz), associated with higher order brain functions such as cognition, perception, and emotion. Phase 1 (P1) (3.5–4.5 Hz) and Phase 2 (P2) (2.5–3.2 Hz) waveforms were examined as previously described (Contreras et al., 2021).

2.3. 5-HT$_{2A}$ and 5-HT$_{2B}$ receptor binding affinity assessment

To assess whether DM506 binds to human 5-HT$_{2A}$ and 5-HT$_{2B}$ receptors, radioligand competition binding experiments were performed as previously described (Luethi et al., 2018) with minor modifications. The results for DM506 were compared with those for DOI, a preferential agonist of 5-HT$_2$ receptors (Pedzich et al., 2022).

Briefly, cell membrane preparations from HEK293 cells expressing the 5-HT$_{2A}$ or 5-HT$_{2B}$ human receptors were incubated with [^{3}H] LSD (1 nM) in the presence of a wide range of concentrations (1 fM-10 μM) of DM506 or DOI in assay buffer (50 mM Tris-HCl, pH 7.4, containing 10 mM $MgCl_2$, 1 mM EGTA) for 1 h at 37 °C. Binding incubations were terminated by rapid filtration through Unifilter-96 plates (PerkinElmer, Schwerzenbach, Switzerland) that were pre-soaked in 0.5% polyethyleneimine. After the addition of Microsint-20 (PerkinElmer) and incubation for 24 h, radioactivity was counted using a TopCount microplate Scintillation Counter (Packard Instrument Company, Meriden, Connecticut, USA). Specific radioligand binding was defined as the difference between total binding (binding buffer alone) and non-specific binding obtained in the presence of 100 μM 5-HT.

The concentration-response data were curve-fitted by non-linear least squares analysis using the Prism software (GraphPad 9.0 Software Inc., La Jolla, CA, USA). The observed IC_{50} values were transformed into inhibition constant (K_i) values using the Cheng–Prusoff relationship (Cheng and Prusoff, 1973):

$$K_i = IC_{50} / \{1 + ([[^3H]LSD]/K_d^{LSD})\} \quad (1)$$

where [[^{3}H]LSD] is the initial concentration of [^{3}H]LSD, and K_d^{LSD} is the dissociation constant for [^{3}H]LSD at the human 5-HT$_{2A}$ and 5-HT$_{2B}$ receptors (2 nM) (Luethi et al., 2018).

2.4. 5-HT$_{2A}$ and 5-HT$_{2B}$ receptor activation assessment

The activity of DM506 on human 5-HT$_{2A}$ and 5-HT$_{2B}$ receptors was compared to that for DOI (Pedzich et al., 2022). Activation of each 5-HT$_2$ receptor subtype was assessed by measuring the accumulation of inositol monophosphate 1 (IP1) using the Cisbio IP-One Gq Kit (Cisbio Bioassays SAS, Codolet Cedex, France), according to the manufacturer's protocol. NIH/3T3 cells transiently transfected with 5-HT$_{2B}$ subunits or stably transfected with 5-HT$_{2A}$ subunits were used. NIH/3T3 cells expressing the respective receptor subtype were seeded at a density of 2500 (5-HT$_{2A}$) or 4000 (5-HT$_{2B}$) cells per well in 384 well plates in Opti-MEM medium (Gibco, ThermoFisher, Life Technologies Europe B.V., Zug, Switzerland). Each test compound was added to the plates and incubated for 90 min at 37 °C, followed by incubation with Anti-IP1-Cryptate and IP1-d2 for 60 min at room temperature. Stimulated IP-1 formation was determined using homogeneous time-resolved fluorescence (HTRF) measurements.

2.5. Statistical analysis

Data were analyzed using Prism 9.0 or SigmaPlot (SYSTAT, Inpixon, Palo Alto, CA, USA). The behavioral and EEG results were analyzed using two-way ANOVA followed by Tukey's (behavior) and Bonferroni's (EEG) post-hoc tests, respectively. The Student's t-test was used to compare the normalized spectral frequency bands. Statistical significance was set at $p < 0.05$.

2.6. Molecular docking and molecular dynamics studies of DM506 and DOI at the 5-HT$_{2A}$ and 5-HT$_{2B}$ receptor

The agonist-bound h5-HT$_{2A}$ [PDB ID: 7WC4; 3.2 Å resolution (Cao et al., 2022a)] and h5-HT$_{2B}$ structures [PDB ID: 7SRQ; 2.7 Å resolution (Cao et al., 2022b)] were refined with the Rosetta cryo-EM relax framework (DiMaio et al., 2013). The 3D structures of DOI and DM506 in the protonated state were used to generate conformers with the BCL (Mendenhall et al., 2021). Molecular docking calculations were run with RosettaLigand (Meiler and Baker, 2006) with the ligand.wts score function. A cubic grid (15 Å × 15 Å × 15 Å) sampling the area close to the Asp residue critical to agonist binding in the 5-HT$_{2A}$ (i.e., D155) and 5-HT$_{2B}$ receptor (i.e., D135) was defined as the orthosteric docking site. The docking poses where the ligand was <6 Å from D155/D135 were kept and only the lowest-scoring poses that formed an interaction with the nitrogen of the ligand and D155 or D135 side chain oxygens were analyzed.

The lowest-scoring docking poses were subjected to 120 ns MD simulations using the AMBER19 software suite (Case et al.). The PPM 2.0 server (Lomize et al., 2012) was used to determine the membrane orientations of the proteins, and CHARMM-GUI (Wu et al., 2014) was used to add water, DOPC lipid molecules, and Cl^- ions at a neutralizing concentration to the system. OPC3 water model (Izadi and Onufriev, 2016), lipid17 lipid model, and ff19SB protein parameters (Tian et al., 2020) were used for the parametrization of the solvated protein/lipid system. The DOI and DM506 molecules were parametrized with the GAFF2 force field (He et al., 2020) with AM1-BCC charges (Jakalian et al., 2002).

The system was minimized in three steps applying restraints to all non-hydrogen atoms in the first step and protein backbone (Cα, C, O, N) atoms and lipid molecules in the second step (10 and 5 kcal/mol Å^2), and with no restraints in the last step. The final structure from the third minimization step was gradually heated and equilibrated in four steps of 5 ns each to a final temperature of 300K in an NVT with restraints on protein backbone Cα, C, O, N atoms, and lipid molecules. The heated system was equilibrated in an NPT ensemble in three 5 ns steps with restraints of 5, 2, and 1 kcal/mol Å^2 on backbone Cα, C, O, N atoms and lipid molecules. Lastly, a 120 ns simulation was run in an NPT environment. All the trajectory analyses and root mean square deviation (RMSD) calculations were run with cpptraj module (Roe and Cheatham, 2013) of AMBER. The RMSD values of the recentered protein were calculated for the 5-HT$_{2A}$ and 5-HT$_{2B}$ simulations with the different ligands over 120 ns with a 0.1 ns step size in reference to the first frame of the NPT production simulation. For the ligand stability, the RMSD and variance values were calculated using non-hydrogen atoms of the ligand between 40 and 120 ns () using the ligand configuration at 40 ns as a reference.

3. Results

3.1. Effect of DM506 on mouse locomotor activity

To assess whether DM506 (15 and 40 mg/kg; i.p.) induced locomotor effects in mice, locomotor activity was measured in the open field 1 h after the drug injection. We tested increasing doses of DM506 to eliminate any interference from locomotor activity in the behavioral tests used in this study. The lowest dose (15 mg/kg) did not induce any locomotor effect, while the higher dose (40 mg/kg) induced a significant decrease in locomotor activity. The effects of only the 15 mg/kg and 40 mg/kg doses are presented. Two-way ANOVA and Tukey's post-hoc analyses indicated a significant decrease in locomotor activity in mice after acute treatment with 40 mg/kg [$F(2, 144) = 114.0$; $p < 0.0001$],

but not with 15 mg/kg DM506 [F (2, 144) = 114.0; p = 0.2807], compared to vehicle-treated mice (Fig. 2).

3.2. DM506 induces anxiolytic-like activity in naïve mice

To determine whether DM506 induces anxiolytic-like activity in naïve mice, the effect of a single (15 mg/kg) or repeated (5 mg/kg) administration at doses with no locomotor effects was assessed using the elevated O-maze test (Fig. 3A). Two-way ANOVA analysis of the results showed that a single administration of 15 mg/kg DM506 significantly decreased the time spent in the closed arms (Fig. 3B) and significantly increased the time spent in the open arms (Fig. 3C) at 1 h, 24 h [F (5, 45) = 80.85; p < 0.0001], 48 h [F (5, 45) = 80.85; p = 0.0003], and 72 h [F (5, 45) = 80.85; p < 0.0043], but not 96 h [F (5, 45) = 80.85; p = 0.99] (for both behaviors), compared to vehicle-treated animals. Volinanserin had no effect on the time spent in open or closed arms compared to animals treated with vehicle [F (1, 72) = 42.98; p = 0,8762] (Fig. 3D). Pre-treatment with volinanserin reduced the marked effects of DM506 at 1 h on the time spent in the open arm [F (1, 72) = 42.98; p = 0.0062] (Fig. 3D). Two-way ANOVA and Tukey's test showed that the effects of DM506 were significantly different at the examined time points. Compared to the effect induced at 24 h, statistical differences were observed at 48 h, 72 h, and 96 h [F (5, 45) = 80.85; p < 0.0001], and compared to the effect at 48 h, statistical differences were observed at 96 h [F (5, 45) = 80.85; p < 0.0003], but not 72 h [F (5, 45) = 80.85; p = 0.962], and a difference was observed between 72 h and 96 h [F (5, 45) = 80.85; p < 0.0034] (Fig. 3B and C).

A lower dose of DM506 (5 mg/kg) did not induce anxiolytic-like activity after acute treatment, specifically after 1 h ([F (2, 54) = 1.429; p = 0.8134]) or 24 h [F (2, 54) = 1.429, p = 0.4611] (Fig. 3E), or after repeated treatment, more precisely after 5 days [F (3, 72) = 4.978; p > 0.99] or 10 days [F (3, 72) = 4.978; p = 0.67]) of treatment (Fig. 3F), compared to vehicle-treated animals. These results indicate that the anxiolytic-like activity of DM506 is dose- and time-dependent, and sensitive to volinanserin.

3.3. DM506 induces anxiolytic-like activity in stressed/anxious mice

To determine whether DM506 induced anxiolytic-like activity in stressed/anxious mice, the effect of a single dose (15 mg/kg, a dose with no locomotor effect) in the absence or presence of volinanserin (0.05 mg/kg) was assessed using the NSFT (Fig. 4A). Two-way ANOVA analysis of the results showed that DM506 significantly reduces the latency to approach the center of the field [F (3, 27) = 45.31; p < 0.0001] (Fig. 4B), and the latency to eat [F (3, 27) = 17.93; p < 0.0001] (Fig. 4C), with the same statistical values at 1 and 24 h compared to vehicle-treated animals. However, no significant changes were observed in in-cage latency to eat [F (3, 27) = 2.026; p = 0.907] (Fig. 4D), or the amount of food consumed during the first 10 min after the NSFT [F (3, 27) = 2.97, p = 0.678] (Fig. 4E). Volinanserin had no effect on the latency to approach the center of the field [F (4, 36) = 34.33; p = 0,5630] (Fig. 4B), latency to eat [F (4, 36) = 16.78; p = 9970] (Fig. 4C), in-cage latency to eat [F (4, 36) = 2.312, p > 0,9999) (Fig. 4D), and food consumption [F (4, 36) = 2.647; p = 0,6301) (Fig. 4E). Pre-treatment with volinanserin reversed the effects of DM506 on the latency to approach the center of the field [F (4, 36) = 34.33; p < 0.0001] (Fig. 4B), and latency to eat [F (4, 36) = 16.78; p = 0.0007] (Fig. 4C), respectively, without changing the in-cage latency to eat [F (4, 36) = 2.312; p = 0.9967] (Fig. 4D), and food consumption [F (4, 36) = 2.647; p = 0.7803] (Fig. 4E). These results showed that DM506 induced anxiolytic-like activity in stressed mice in a volinanserin-sensitive manner with no notable reduction in food intake.

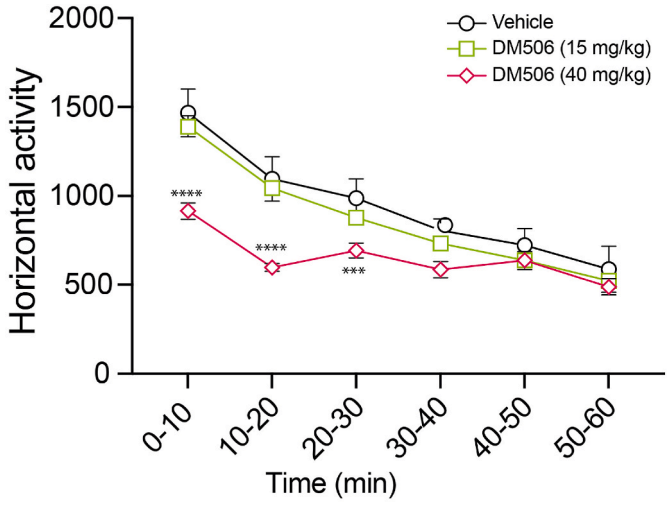

Fig. 2. Effect of DM506 on locomotor activity and head-twitch response in mice. (A) Mice (n = 10/condition) were injected with DM506 (base) (15 or 40 mg/kg; i.p.), or vehicle, and the locomotor activity was recorded every 10 min for 1 h in the open field. Statistical analyses showed a significant decrease in mouse locomotor activity after acute treatment with 40 mg/kg (⋄) (***p < 0.005; ****p < 0.0001), but not 15 mg/kg DM506 (£) (p = 0.7349), compared to vehicle-treated mice (¡).

3.4. Sedative activity of DM506 in naïve mice

Since 40 mg/kg DM506 decreased locomotor activity (see Fig. 2), we tested the hypothesis that DM506 could induce sedative/hypnotic effects in naïve mice. In this regard, the sedative-like effect of 15 and 40 mg/kg DM506 was subsequently investigated in the absence and presence of volinanserin (0.05 mg/kg; s.c.) using the LORR test (Fig. 5A). Two-way ANOVA analysis of the results showed that DM506 at 40 mg/kg [F (4, 36) = 5.592; p = 0.0029], but not at 15 mg/kg [F (4, 36) = 5.592; p = 0.9823], significantly induces a loss of righting reflex compared to vehicle-treated animals (Fig. 5B). Pre-treatment with volinanserin reversed the effects of 40 mg/kg DM506 [F (4, 36) = 5.592; p = 0.0147] (Fig. 5B).

3.5. Effect of DM506 on head-twitch response

The head-twitch response is a repetitive, sudden rotation of the head observed in rodents following treatment with a range of 5-HT_{2A} receptor agonists that induce hallucinogenic activity such as LSD, DOI, and TBC-2 (Halberstadt, 2015). Drug-induced head-twitch serves as a practical mice model to determite a possible hallucinogenic activity in humans (Fantegrossi et al., 2010). In this study, we investigated whether DM506 (10, 15, 25, and 40 mg/kg; i.p.) induces head twitches in mice. We compared the activity of DM506 with that induced by TBC-2 (1 mg/kg) and DOI (1 mg/kg) (Fig. 6), which are compounds that produce head twitching effects (Fox et al., 2010). Our results showed that both TBC-2 and DOI induce head twitches in mice with statistically similar values [F (6, 63) = 999.5; p < 0.0001)], while DM506 has no significant effect at 10 or 15 mg/kg [F (6, 63) = 999.5; p > 0.999)], 25 mg/kg [F (6, 63) = 999.5; p = 0.615)], and 40 mg/kg [F (6, 63) = 999.5; p = 0.315)], respectively.

3.6. 3.6. DM506 elevates electroencephalogram delta (δ) power while suppressing gamma (γ) power

To investigate the effects of DM506 on brain activity, we performed EEG recordings in mice. Representative traces suggest that administration of 15 mg/kg DM506 fumarate caused an increase in the power of the low-frequency EEG spectra (Fig. 7A). Low-frequency EEG spectra represent slow and synchronized brain activity, with the FFT (fast Fourier transform) power of the EEG signal reflecting the relative size of the neuronal field, as well as the synchronicity of neuronal contributions

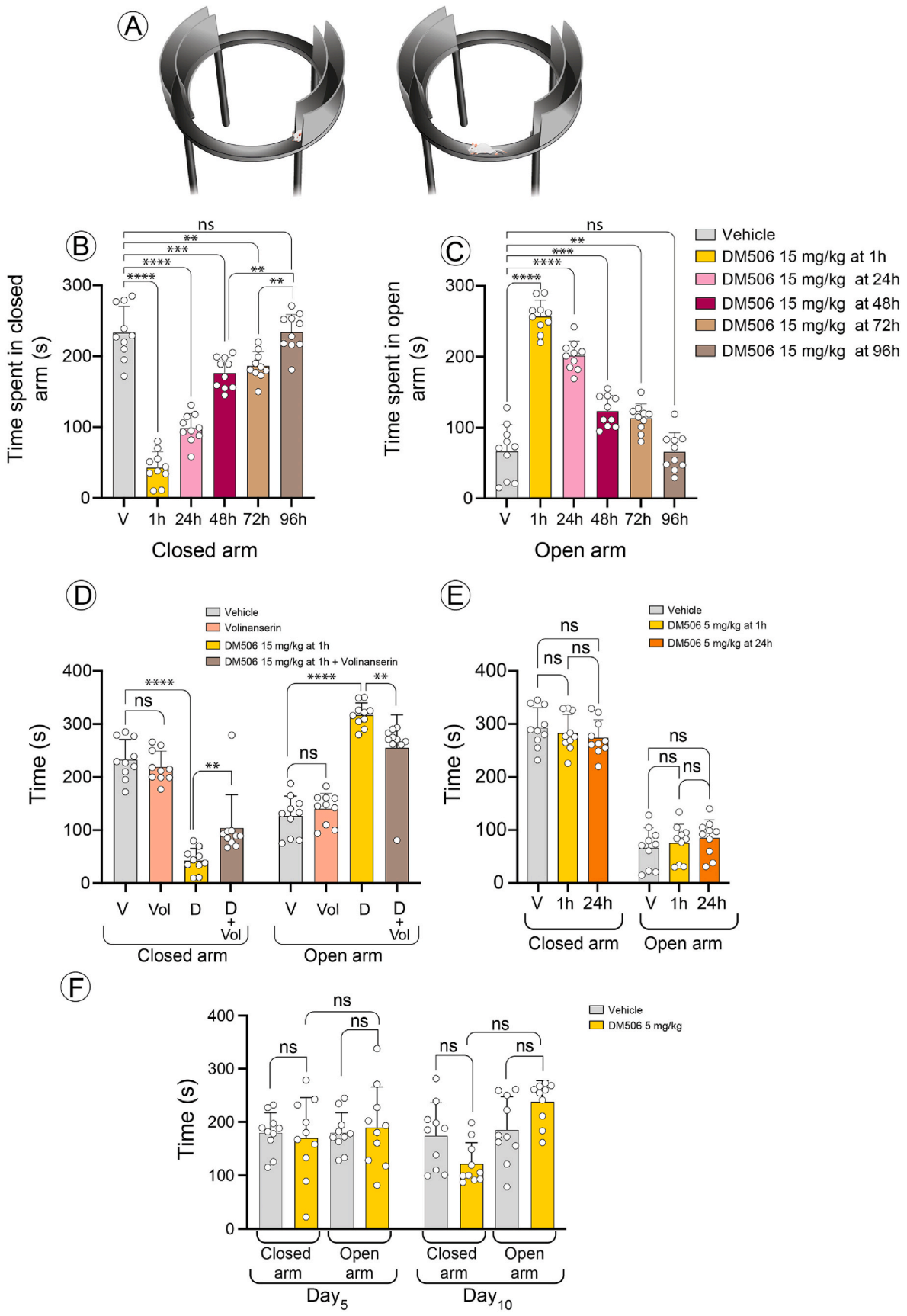

(caption on next page)

Fig. 3. Anxiolytic-like activity of DM506 after single and repeated treatment of naïve mice using the O-maze test. Mice (n = 10/condition) were injected (i.p.) with a single dose (15 mg/kg) of DM506 (base), or vehicle, and the anxiolytic-like activity was determined at 1 h and 24 h (acute effect), and at 48 h, 72 h, and 96 h (long-lasting effect). To determine the role of the 5-HT_{2A} receptor, volinanserin (Vol) (0.05 mg/kg; s.c.) was injected 15 min before DM506. (B,C) Statistical analysis of the results showed that a single dose of 15 mg/kg DM506 significantly decreased the time spent in closed arms (B) and significantly increased the time spent in open arms (C) at 1 h, 24 h ($p < 0.0001$), 48 h ($p = 0.0003$), and 72 h ($p = 0.0043$), but not at 96 h ($p = 0.9999$) (for both behaviors), compared to vehicle-treated animals. The effects of DM506 were significantly different at the time points studied. Compared to the effect induced at 24 h, statistical differences were observed at 48 h, 72 h, and 96 h ($p < 0.0001$), as well as the differences between 48 h ($p < 0.0003$) or 72 h ($p < 0.003$) and 96 h, respectively. (D) Volinanserin, when used alone, had no effect on the time spent in open or closed arms compared to animals treated with vehicle with the same statistical values [$F (1, 72) = 42.98$; $p = 0,8762$]. (D) Pre-treatment with volinanserin reversed the effects of DM506 at 1 h on time spent in closed and open arms, with the same statistical values [$F (1, 72) = 42.98$; $p = 0.0062$). (E,F) Another group of mice was treated with a lower dose (5 mg/kg) of DM506, or vehicle, for 10 consecutive days (repeated treatment), and the anxiolytic-like activity was determined on day 5 (Day_5) and day 10 (Day_{10}), respectively. Statistical analysis showed that DM506 does not induce significant changes in the time spent in the closed and open arms, respectively, after acute [i.e., 1 h or 24 h ($p > 0.46$)] (E) or repeated treatment [i.e., 5 or 10 days ($p > 0.22$)] (F), compared to vehicle-treated animals. **$p < 0.01$; ***$p < 0.001$; ****$p < 0.0001$.

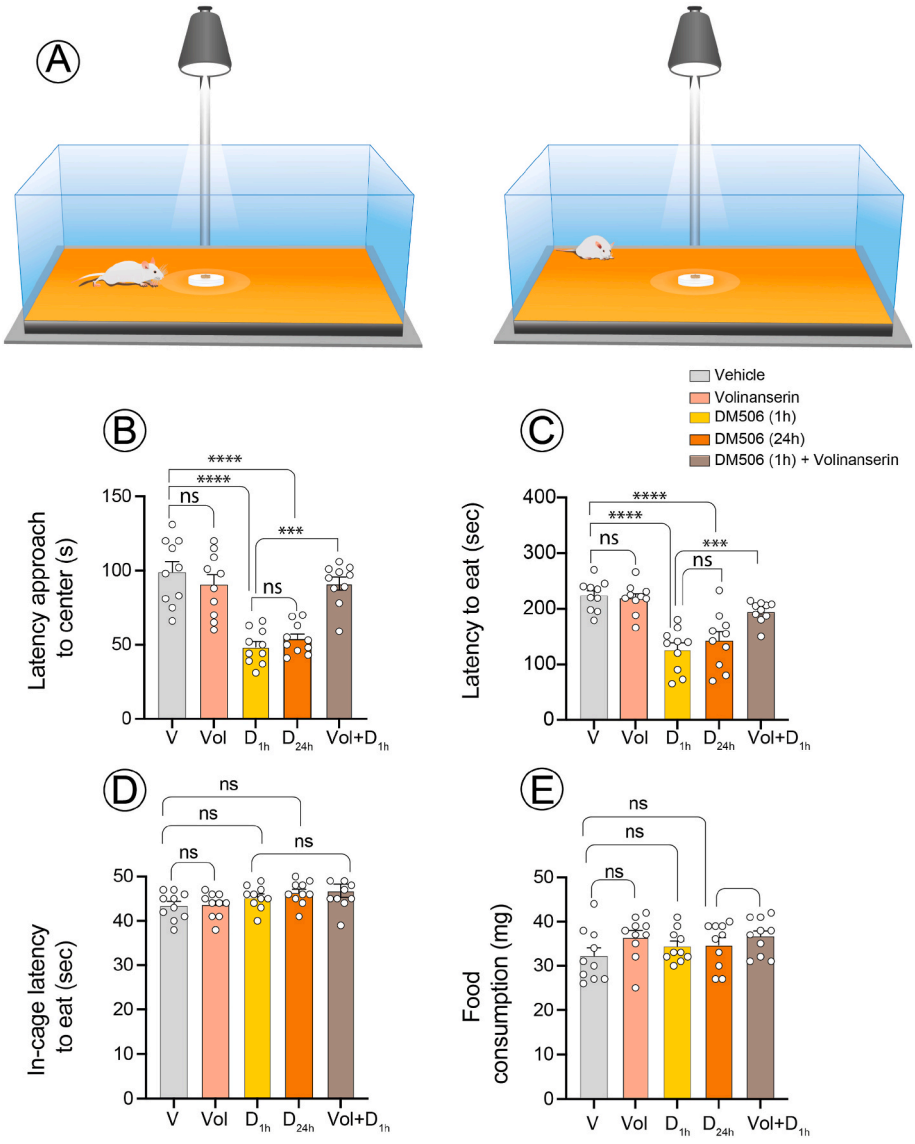

Fig. 4. Anxiolytic-like activity of DM506 in stressed/anxious mice using the novelty feed test (NSFT). After 24 h of food deprivation, mice (n = 10/condition) were injected (i.p.) with a single dose (15 mg/kg) of DM506 (base), or vehicle. The 5-HT_2 antagonist volinanserin (0.05 mg/kg) was administered (s.c.) 15 min before DM506 (A) Scheme of the apparatus. Two-way ANOVA analysis of the results showed that DM506 significantly reduced the latency to approach the center of the field ($p < 0.0001$) (B) and latency to eat ($p < 0.0001$) (C), with same statistical values at 1 h and 24 h, compared to vehicle-treated animals. Volinanserin, when used alone, had no effect on the latency to approach the center of the field [$F (4, 36) = 34.33$; $p = 0,5630$] (Fig. 3B), on latency to eat [$F (4, 36) = 16.78$; $p = 9970$] on in-cage latency to eat [$F (4, 36) = 2.312$, $p > 0,9999$) and on food consumption [$F (4, 36) = 2.647$; $p = 0,6301$). Pre-treatment with volinanserin reversed the effects of DM506 on latency to approach the center of the field ($p < 0.0001$) (B) and latency to eat ($p = 0.0006$) (C). On the other hand, no significant changes were observed for in-cage latency to eat ($p = 0.9075$) (D) or the amount of food consumed during the first 10 min after the NSFT ($p = 0.6785$) (E) at 1 h and 24 h, compared to vehicle-treated animals. In addition, volinanserin had no effect on in-cage latency to eat ($p = 0.7479$) (D) and food consumption ($p = 0.7136$) (E), respectively. ***$p < 0.001$; ****$p < 0.0001$.

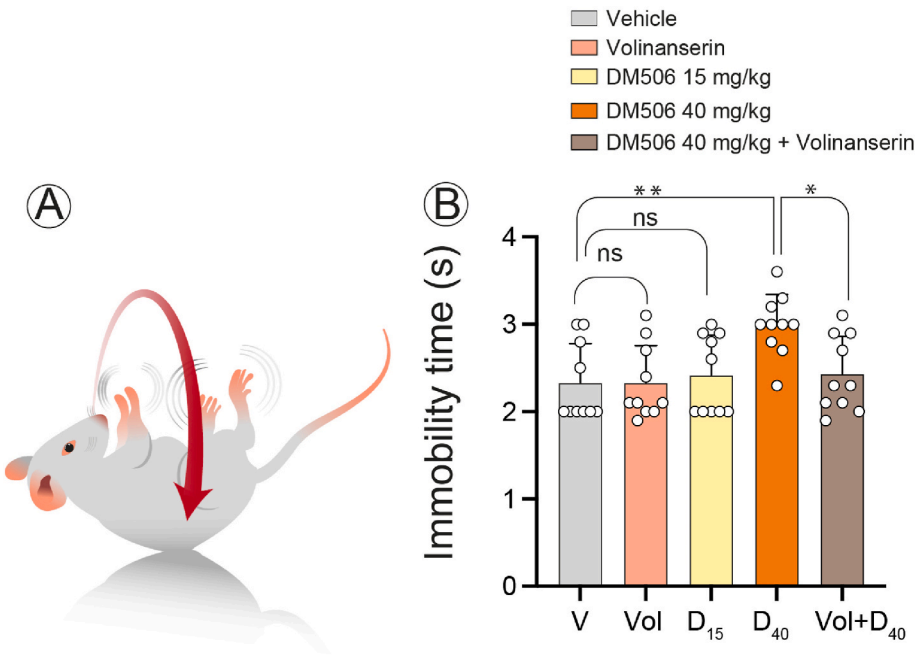

Fig. 5. Sedative-hypnotic activity of DM506 on naïve mice. Mice (n = 10/condition) were injected (i.p.) with 15 or 40 mg/kg DM506 (base), or vehicle, and the immobility time was subsequently determined using the loss of righting reflex (LORR) test (A). Volinanserin (0.05 mg/kg; s.c.) was administered 15 min before DM506. Statistical analysis showed that DM506 at 40 mg/kg ($p = 0.0029$) but not at 15 mg/kg ($p = 0.9823$) significantly induces a loss of righting reflex (B), compared to vehicle-treated animals. Pre-treatment with volinanserin reversed the effects of DM506 at 40 mg/kg ($p = 0.0147$). *$p < 0.05$; **$p < 0.001$. Volinanserin, used alone, had no sedative effect ($p > 0,9999$).

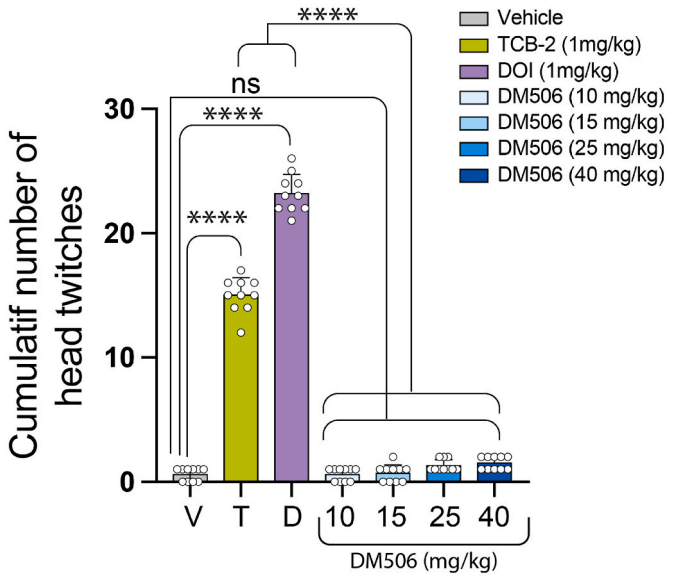

Fig. 6. Effect of DM506 on head-twitch response. Mice (n = 10/condition) were injected (i.p.) with DM506 (base) (10, 15, 25, or 40 mg/kg; i.p.), or vehicle, and the head-twitch response compared to that for the hallucinogenic agents TBC-2 (1 mg/kg; i.p.) and DOI (1 mg/kg; i.p.), respectively. Statistical analyses showed that both TBC-2 and DOI induced head-twitch responses in mice with statistically similar levels (****$p < 0.0001$), whereas DM506 had no significant (ns) effect at the different doses studied ($p > 0.314$).

(Greene and Frank, 2010). The spectrogram supports the elevation of low-frequency power, as well as the suppression of power in the high-frequency range by DM506 (darker blue near the top of the spectrogram; Fig. 7B). Quantitative comparison of raw δ power between baseline and DM506 showed a progressive increase in δ frequency range power over the 1-h recording period (Fig. 7C). Two-way ANOVA and Bonferroni's post-hoc analyses revealed a significant interaction between treatment and time ($p < 0.001$), and a significant effect of treatment ($p = 0.014$).

Spectral analysis showed that the normalized δ power was significantly increased by DM506 compared to that at the baseline (Fig. 7D; Student's t-test, $p < 0.001$). It is well established that the δ power increases during slow-wave NREM sleep states, reflecting synchronized oscillatory neocortical activity (Greene and Frank, 2010). In contrast, the normalized power in θ (Fig. 7E), α (Fig. 7F), and β (Fig. 7G) frequency ranges were not affected by DM506 compared to the baseline ($p > 0.05$). Theta is seen during REM sleep states as well as during conscious states of spatial navigation. Alpha frequency band activity is commonly observed during quiet wakes, whereas higher-frequency β-wavelength activity is observed during focused effort or concentration. In contrast to δ, we found that the normalized γ power was significantly suppressed by DM506 compared to the baseline (Fig. 7H; Student's t-test, $p < 0.001$). Gamma wavelength activity is associated with increased arousal and higher order brain functions, including cognition, perception, and emotion (Oathes et al., 2008).

We also investigated the characteristics of waveforms induced by DM506. The results showed that DM506 produced both characteristic waveforms P1 (2–4.5 Hz) and P2 (1–2.5 Hz) (Fig. 7I and J). However, P1 was much greater than P2, especially during the first 30 min [Student's t-test, $p = 0.029$ (Fig. 6K); $p = 0.005$ (Fig. 6L)]. P1 is characterized by a lack of muscle activity, whereas P2 is associated with strong muscle contractions (Contreras et al., 2021). The higher incidence of P1 waveforms may be related to the decreased locomotor activity observed at higher DM506 doses (Fig. 2). In general, EEG spectral frequency analysis suggested that DM506 produces a sedative/hypnotic-like state by increasing the synchronization and power in the δ wavelength, and the P1 waveform, with a concomitant shift away from power in the fast γ wavelength.

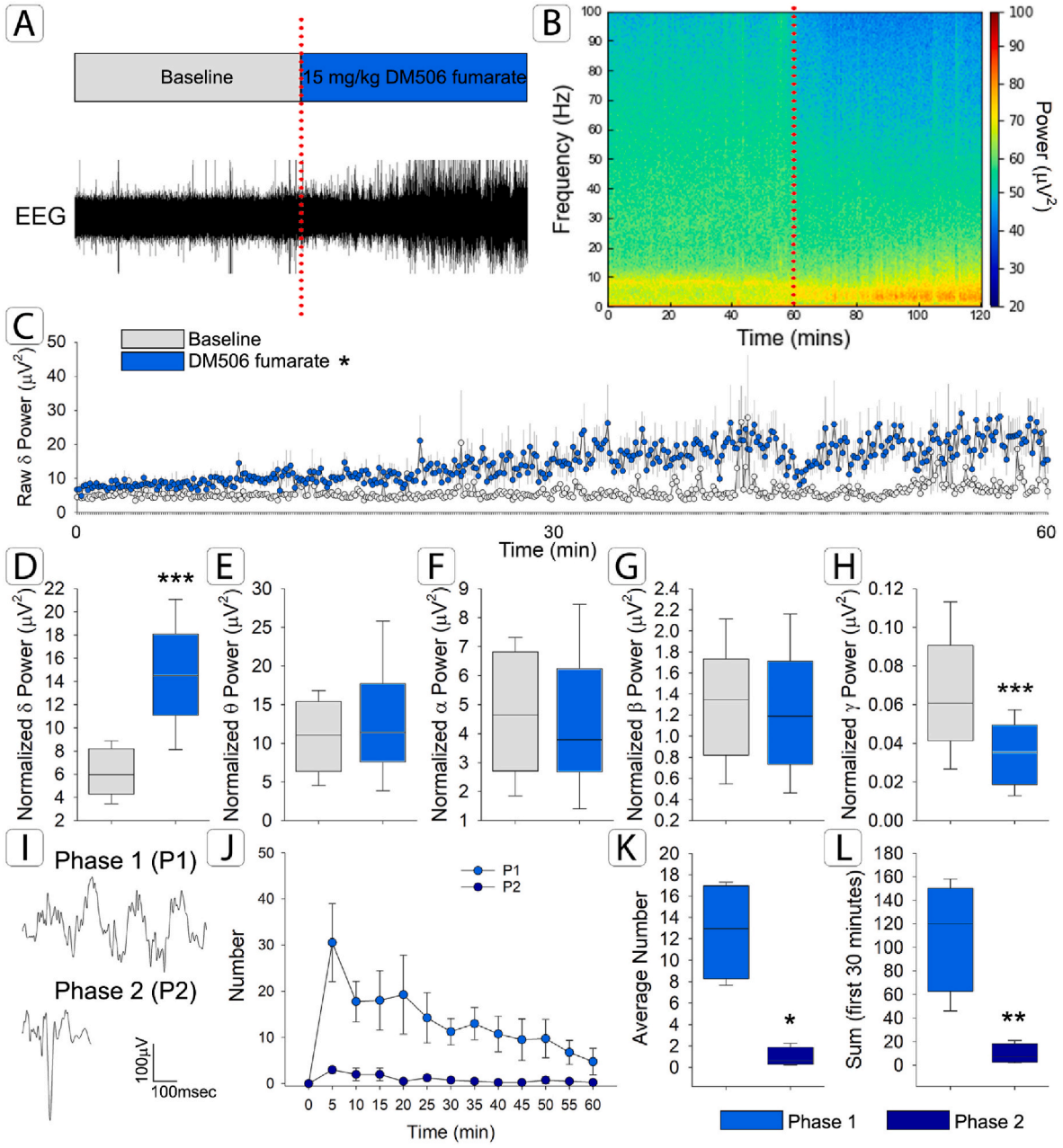

Fig. 7. Effect of DM506 on electroencephalogram (EEG) activity. (A) Representative EEG traces during the baseline and after administration of 15 mg/kg DM506 fumarate. The red line indicates the time of injection (i.p.). (B) Representative spectrogram of EEG activity over time, showing the power (color spectra) by frequency. (C) Raw power in the δ frequency range, showing the progressive increase in power after DM506 treatment compared to the baseline (n = 8; mean ± SD). Statistical analysis showed significant interaction between treatment and time ($p < 0.001$) and significant effect of treatment ($p < 0.05$). (D) Comparison of normalized δ frequency domain power between DM506 and baseline ($p < 0.001$). (E–H) Comparison of normalized θ (E), α (F), β (G), and γ (H) frequency domain power between DM506 and baseline. Gamma frequency range power was significantly decreased by DM506 compared to the baseline ($p < 0.001$). (I) Representative traces of Phase 1 (P1) and Phase 2 (P2) waveforms following DM506 treatment. (J) Analysis of the number of P1 and P2 waveforms over time following DM506 treatment. (K) Statistical analysis showed that DM506 significantly increases the number of P1 waveforms compared to P2 waveforms ($p < 0.05$). (L) P1 waveforms predominate especially during the first 30 min ($p < 0.01$). Graphs plot median with the first and third quartile, and whiskers show minimum and maximum (D-H, K, L), or mean ± SD (C, J).

3.7. Effect of DM506 on human 5-HT$_{2A}$ and 5-HT$_{2B}$ receptors compared with DOI

To assess the pharmacological effects of DM506 on 5-HT$_{2A}$ and 5-HT$_{2B}$ receptors, the binding affinity (Fig. 8) and functional activity (Fig. 9) of this compound were evaluated and compared with those of the potent psychedelic compound DOI (Table 1). Radioligand competition binding experiments using [^{3}H]LSD as a probe for the orthosteric site showed that DM506 binds to the 5-HT$_{2B}$ receptor with a slightly lower inhibitory constant (K_i = 16.5 nM) than that for the 5-HT$_{2A}$ receptor (24.1 nM), indicating a binding affinity that is approximately 4- and 12-fold weaker than that for DOI (3.6 and 2.0 nM, respectively) (Table 1).

Since the binding affinity does not distinguish between agonist and antagonist activity, the functional properties of DM506 were compared to those of DOI in both receptor subtypes (Fig. 9). DM506 did not inhibit, but activated, the 5-HT$_{2A}$ receptor with lower potency (EC_{50} = 9 nM) than DOI (0.23 nM) (Table 1). Although DOI fully activated the 5-HT$_{2A}$

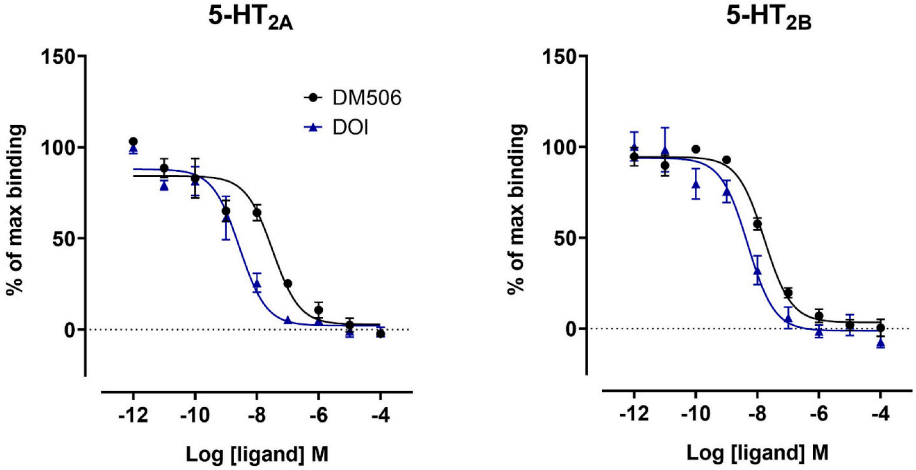

Fig. 8. Radioligand competition binding experiments for DM506 and DOI at human 5-HT_{2A} and 5-HT_{2B} receptors. HEK293 cell membranes containing each separate receptor subtype were incubated (1 h) with 1 nM [^{3}H]LSD and an ample range of DM506 (●) and DOI (▲) concentrations, respectively. Non-specific binding was determined at 100 μM 5-HT. Data are presented as mean ± SEM from three experiments, each performed in duplicate. The IC_{50} values, obtained by non-linear least squares fit, were used to calculate the K_i values [Eq. (1)], which are summarized in Table 1.

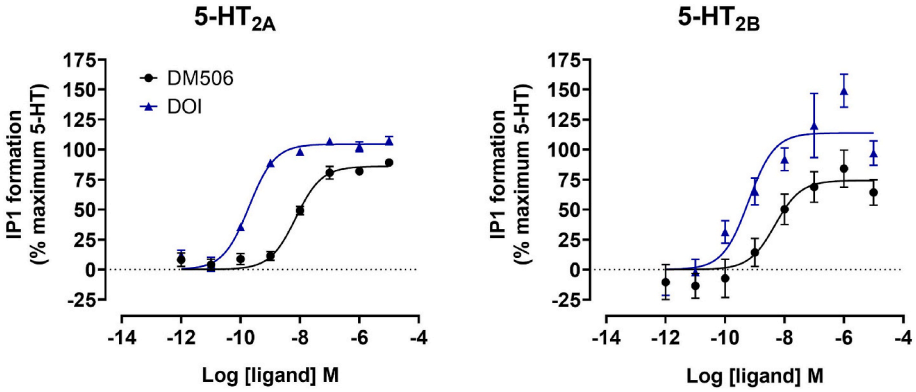

Fig. 9. Effect of DM506 and DOI on human 5-HT_{2A} and 5-HT_{2B} receptors. NIH/3T3 cells expressing each receptor subtype were incubated (1 h) with a wide range of DM506 (●) or DOI (▲) concentrations. Activation of each receptor was assessed by IP1 formation using Homogeneous Time Resolved Fluorescence (HTRF) measurements. Receptor activation raw data were normalized with 0% representing the baseline signal and 100% representing the maximum 5-HT-stimulated signal at the respective receptor. Data are presented as mean ± SEM from at least three experiments, each performed in triplicate. The EC_{50} and E_{max} values are summarized in Table 1.

Table 1
Binding affinity (K_i), activation potency (EC_{50}), and activation efficacy (E_{max}) of DM506 and DOI at human 5-HT_{2A} and 5-HT_{2B} receptors.

Receptor Subtype	Compound	K_i (nM) [95% CI]	EC_{50} (nM) [95% CI]	E_{max} (%)
5-HT_{2A}	DM506	24.1 [10.3–52.6]	9.0 [5.7–12.7]	76 ± 16
	DOI	2.0 [1.0–4.3]	0.23 [0.16–0.33]	101 ± 1
5-HT_{2B}	DM506	16.5 [8.8–18.6]	2.9 [0.65–13.5]	69 ± 4
	DOI	3.6 [1.6–8.2]	0.62 [0.15–2.2]	130 ± 4

K_i values were calculated using Eq. (1), whereas EC_{50} (potency) and E_{max} (efficacy) values were calculated using the HTRF values. E_{max} percentages were obtained considering 100% activation by 5-HT.

receptor (E_{max} = 101 ± 1% compared to the full agonist 5-HT), it was partially activated by DM506 (E_{max} = 76 ± 16%). The activating potency of DM506 (2.9 nM) on the 5-HT_{2B} receptor was also lower than that of DOI (0.62 nM), with DM506 only partially activating this receptor subtype (69 ± 4%) compared to complete activation by DOI (130 ± 4%). It was concluded from these experiments that DM506 behaves as a potent partial agonist of both the 5-HT_{2A} and 5-HT_{2B} receptor subtypes.

3.8. Molecular docking and molecular dynamics simulations for DM506 and DOI at the 5-HT_{2A} and 5-HT_{2B} receptor models

Our molecular docking results showed that both DM506 and DOI bind to the agonist site of each 5-HT_{2A} (Fig. 10A) and 5-HT_{2B} (Fig. 10B) receptor model, with the charged nitrogen group from each molecule forming an ionic interaction with the respective negative charges of D155/D135, and the remainder of the molecule interacting with various hydrophobic residues (Table 2). Some of the 5-HT_{2B} residues interacting with DM506 (e.g., D135, M218, and A225) were also observed with LSD (Cao et al., 2022a).

The RMSD values measured from the MD simulations (Fig. 10A and B) were relatively small and with variance below 0.4 Å (Table 2), suggesting stable docking of both DM506 and DOI to each model. The RMSD value for DM506 at the 5-HT_{2B} receptor was lower than that for DOI (Table 2), suggesting that the DOI docking was relatively less stable, potentially due to its more flexible nature. The critical interactions with D155/D135 (Cao et al., 2022a) on the respective receptor were conserved over the simulations (Table 2). The most important difference

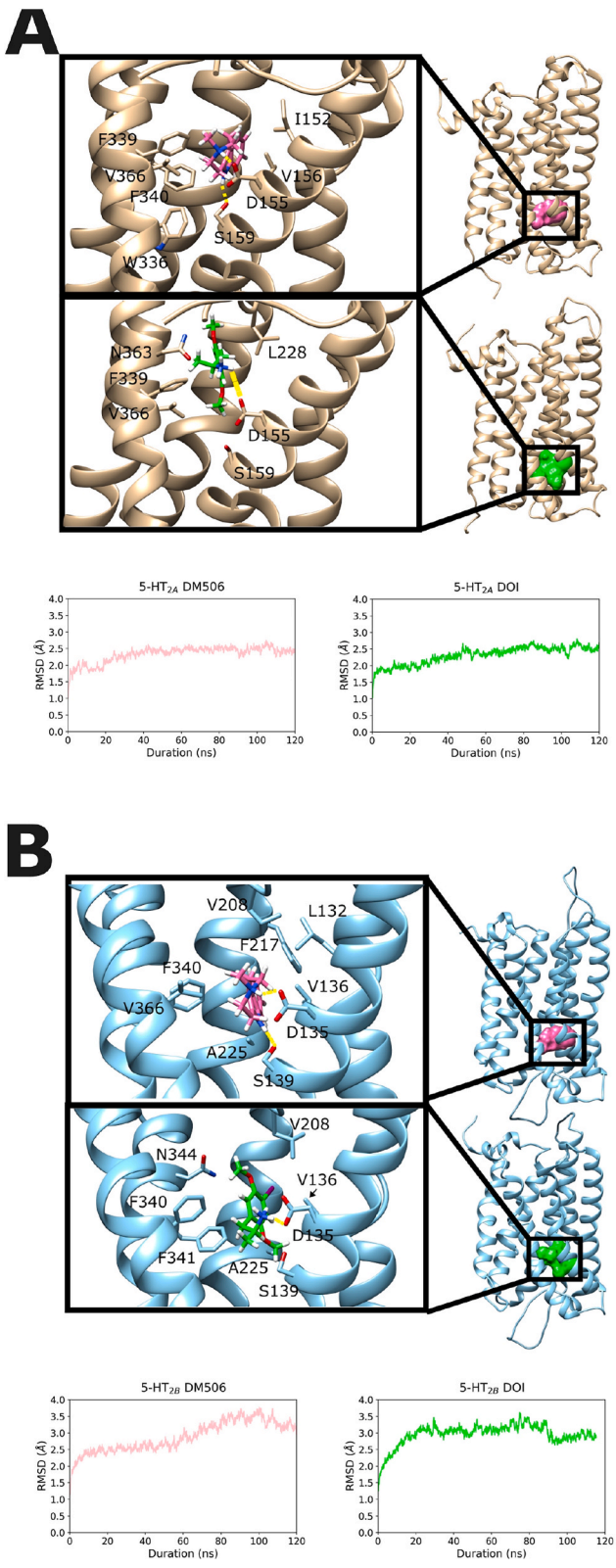

Fig. 10. Molecular docking and molecular dynamics of DM506 and DOI to the human 5-HT$_{2A}$ and 5-HT$_{2B}$ models. Closeup of the docking poses for DM506 (fuchsia) and DOI (green) at the 5-HT$_{2A}$ (A) and 5-HT$_{2B}$ (B) model. Each ligand formed ionic interactions with D135/D155, whereas only DM506 formed hydrogen bonding with S159/S139 (highlighted in yellow). Additional details of the molecular interactions of both ligands were summarized in Table 2. The bottom panels show the RMSD plots (120 ns simulation) for DM506 (fuchsia) and DOI (green) at each 5-HT$_{2A}$ (A) and 5-HT$_{2B}$ (B) model.

Table 2
Molecular docking and molecular dynamics of DM506 and DOI at the human 5-HT$_{2A}$ and 5-HT$_{2B}$ receptor models.

Compound	5-HT$_{2A}$ receptor model		5-HT$_{2B}$ receptor model	
	RMSD (variance) (Å)	Interacting Residues	RMSD (variance) (Å)	Interacting Residues
DM506	0.31 (0.07)	I152, **D155**, V156, *S159*, T160, L229, S242, W336, F339, F340, V366	0.24 (0.06)	L132, **D135**, V136, *S139*, T140, L209, M218, A225, W337, F340, V366, Y370
DOI	0.39 (0.08)	I152, **D155**, V156, S159, I210, S242, W336, F339, F340, V366, Y370	0.37 (0.07)	**D135**, V136, S139, T140, L209, M218, A225, W337, F340, F341, N344, V366, Y370

was the restructuring of 5-HT$_{2A}$-TM5, whereby F243 and F340 formed a π-π stacking interaction (Fig. 10A). A similar interaction was already present in the 5-HT$_{2B}$ structure used for the docking calculations, which was retained over the 120 ns simulation.

Although both compounds docked to the same agonist binding sites, subtle differences were observed between them. DM506 formed hydrogen bonding with both 5-HT$_{2A}$-S159 (Fig. 10A) and 5-HT$_{2B}$–S139 (Fig. 10B), whereas these interactions were not observed for DOI (Table 2). The simulations of DOI were also different between the 5-HT$_{2A}$ and 5-HT$_{2B}$ models in terms of the placement of the alkyl ring bearing the primary amine group and the aromatic ring bearing the iodine atom. DOI was buried deeper into the 5-HT$_{2B}$ binding cavity where its methoxy methyl group interacted with the S139 side chain (Fig. 10B). In addition, the DOI iodine moiety pointed toward 5-HT$_{2A}$-G238 (Fig. 10A).

Ligand stability was measured as the RMSD (variance) values obtained between 40 and 120 ns of the MD simulation as explained in the Methods section. Smaller values indicate higher docking stability.

Residues in **bold** indicate ionic interactions. Residues in *italics* indicate hydrogen bonding.

4. Discussion

The main objective of this study was to determine the anxiolytic- and sedative-like activities of DM506 in naïve and stressed/anxious mice after acute and repeated treatments. Additional EEG, functional, radioligand binding, and molecular docking studies were performed to determine the plausible molecular mechanisms underlying the observed behavioral activities.

The results from the elevated O-maze test showed that a single dose (15 mg/kg) of DM506 (base) induces acute (1–24 h) and long-lasting (48–72 h) anxiolytic activity in naïve mice. The acute effect was sensitive to volinanserin and did not affect locomotor function in mice. Repeated administration of 5 mg/kg DM506 did not induce cumulative anxiolytic-like activity or side effects (e.g., tremorgenic or locomotor effects). The results of the NSFT showed that 15 mg/kg DM506 produces acute (1–24 h) anxiolytic-like activity in stressed/anxious mice in a volinanserin-sensitive manner, without altering feeding habits. The LORR study showed that DM506 could also induce sedative/hypnotic effects at higher doses (40 mg/kg). Volinanserin is an antagonist with high selectivity for 5-HT$_{2A}$ receptors ($K_i = 0.5$ nM) compared to that for other 5-HT$_2$ and 5-HT$_1$ receptors ($K_i > 0.1$ μM) (Casey et al., 2022). Given that DM506 induces sedative- and anxiolytic-like activities in a volinanserin-sensitive manner, it is likely that the 5-HT$_{2A}$ receptor subtype is involved in these behavioral effects. However, we cannot completely rule out the possibility that 5-HT$_{2B}$ or other receptor

subtypes are also involved in the observed effects.

Previous studies have shown that TBG fumarate, derived from tabernanthine (Cameron et al., 2021), induces acute (24 h) anxiolytic-like activity and cognitive flexibility in mice under unpredictable mild stress conditions (Lu et al., 2021). These behavioral effects coincide with dendritic spine regrowth and excitability of inhibitory interneurons (Cameron et al., 2021; Lu et al., 2021), supporting the notion that the anxiolytic and procognitive activity of TBG is mediated by morphological and functional changes in those neurons. Our results showed that DM506 induces long-lasting anxiolytic-like activity (>24 h), supporting new therapeutic perspectives for ibogalog compounds as non-benzodiazepine sedatives.

To further investigate the pharmacological activity of DM506, its binding affinity, functional activity, and docking properties at each 5-HT_{2A} and 5-HT_{2B} receptor were evaluated and compared with those for DOI (Pedzich et al., 2022). Radioligand competition binding experiments showed that DM506 binds to 5-HT_{2B} (24 nM) and 5-HT_{2A} (16 nM) receptors with 4-fold and 12-fold lower affinities, respectively, than DOI. The functional results showed that DM506 activates both 5-HT_{2A} and 5-HT_{2B} receptors with potency (9.0 and 2.0 nM, respectively) and efficacy (76 and 69%, respectively) lower than those of the full agonist DOI (Pedzich et al., 2022). The molecular docking and molecular dynamics results showed that DM506 binds to the agonist site of both 5-HT_{2A} and 5-HT_{2B} receptors in a stable manner and similar fashion to that determined for DOI. Both ligands formed ionic interactions with the critical D155/D135 residues at each receptor (Cao et al., 2022a), whereas only DM506 formed hydrogen bonding with S159/S139. These functional and structural results indicate that DM506 is a potent partial agonist of both 5-HT_{2A} and 5-HT_{2B} receptors.

Our EEG study provides further information supporting the role of the 5-HT_{2A} receptor subtype in the anxiolytic/sedative-like activity of DM506. Previous EEG results have shown that the selective activation of the 5-HT_{2A} receptor by 25I–NBOH produces a two-waveform complex, P1 (3.5–4.5 Hz) and P2 (2.5–3.2 Hz), with a higher incidence of the former (Contreras et al., 2021). P1 is considered to be a hallmark of behavioral arrest [i.e., **temporary cessation of movement of the whole body (**Klemm, 2001**);]**, whereas P2 is associated with the head-twitch response observed with hallucinogenic compounds (Contreras et al., 2021). The finding that DM506 had a comparatively lower incidence of P2 waveforms is consistent with the present and previous (Cameron et al., 2021) studies showing that ibogalogs activate 5-HT_{2A} receptors without head-twitch responses. EEG spectral frequency analysis showed that DM506 increased the transition from a highly alert state (i.e., fast γ wavelength) to a more synchronized deep sleep activity (i.e., δ wavelength), without affecting the α, θ, and β bands. In contrast, hallucinogenic agents such as LSD and psilocybin decreased the low α and θ bands (Pallavicini et al., 2019) indicating an important difference with DM506 and perhaps other non-hallucinogenic compounds.

A highly alert or hyperarousal state is a primary symptom observed in patients with post-traumatic stress disorder (PTSD), which is the basis for recurrent, long-lasting stress/anxiety effects (Sherin and Nemeroff, 2011). On the other hand, slow-wave sleep is essential for the homeostatic connections between the autonomic nervous and endocrine systems (Besedovsky et al., 2022; Leger et al., 2018). Therefore, our results support further studies to determine the potential use of DM506 for the treatment of PTSD and insomnia.

Numerous studies have been conducted on 5-HT_{2A} receptor agonists that induce head-twitch responses in rodents, which is considered as a proxy of hallucinogenic activity (Moreno et al., 2011). The role of the 5-HT_{2A} receptor in this behavioral activity has been based on the blocking action of selective 5-HT_{2A} receptor antagonists, and the lack of response in 5-HT_{2A} receptor knockout mice (Gonzalez-Maeso et al., 2007). Nevertheless, some compounds activate the 5-HT_{2A} receptor with no head twitch response or show persistent head twitch response, even in the presence of a selective blocker (Gonzalez-Maeso et al., 2007). Although DM506 behaved as a potent 5-HT_{2A} agonist, it did not induce head-twitch responses in mice at the doses studied. Thus, DM506, TBG, and IBG (Cameron et al., 2021) can be considered new members of the 5-HT_{2A} receptor agonist subfamily presumably devoid of hallucinogenic properties in humans. A simple explanation for this lack of head twitch response is based on the reduction of the head-twitch response by 5-HT_{2C} receptor agonists (Fantegrossi et al., 2010; Serafine et al., 2015). However, the non-hallucinogenic compounds TBG/IBG are potent 5-HT_{2C} receptor antagonists (Cameron et al., 2021). There is new experimental evidence indicating that the hallucinogenic *vs* non-hallucinogenic property is mediated by distinct intracellular pathways (Cumming et al., 2021; Lopez-Gimenez and Gonzalez-Maeso, 2018). Although the activation of the 5-HT_{2A} receptor stimulates the $G_{\alpha q}$-induced phospholipase C pathway, hallucinogens may also stimulate the phospholipase A_2 and $G_{i/o}$-dependent pathways (Kurrasch-Orbaugh et al., 2003; Moya et al., 2007). It is plausible that the absence of head-twitch response by DM506 and TBG/IBG (Cameron et al., 2021) is based on the lack of selective $G_{i/o}$-dependent activation.

In conclusion, our study represents a pioneering exploration of the anxiolytic and sedative potential of DM506 in mouse models. This study provides evidence that DM506 produces both acute and long-lasting anxiolytic- and sedative-like effects, primarily through a mechanism that enhances the induction of a sleep state without hallucinogenic effects, likely mediated by 5-HT_{2A} receptor activation.

CRediT authorship contribution statement

Hugo R. Arias: Writing – review & editing, Writing – original draft, Visualization, Validation, Supervision, Conceptualization. **Deborah Rudin:** Investigation, Formal analysis. **Dustin J. Hines:** Formal analysis. **April Contreras:** Formal analysis. **Alican Gulsevin:** Software, Methodology. **Dina Manetti:** Investigation. **Youssef Anouar:** Writing – original draft. **Philippe De Deurwaerdere:** Writing – review & editing, Visualization, Validation, Formal analysis. **Jens Meiler:** Software, Methodology. **Maria Novella Romanelli:** Investigation. **Matthias E. Liechti:** Writing – review & editing. **Abdeslam Chagraoui:** Writing – review & editing, Writing – original draft, Visualization, Validation, Supervision, Conceptualization.

Declaration of Competing Interest

We wish to confirm that there are no known conflicts of interest associated with this publication and there has been no significant financial support for this work that could have influenced its outcome.

Data availability

Data will be made available on request.

Acknowledgements

This research was supported by the University of Florence Fondo Ricerca Ateneo RICATEN22, Italy (to MNR and DM), and OVPR Pilot/Seed Grants (Oklahoma State University Center for Health Sciences) (to HRA).

References

Arias, H.R., De Deurwaerdere, P., El-Kasaby, A., Di Giovanni, G., Eom, S., Lee, J.H., Freissmuth, M., Chagraoui, A., 2023a. (+)-Catharanthine and (-)-18-methoxycoronaridine induce antidepressant-like activity in mice by differently recruiting serotonergic and norepinephrinergic neurotransmission. Eur. J. Pharmacol. 939, 175454 https://doi.org/10.1016/j.ejphar.2022.175454.

Arias, H.R., De Deurwaerdere, P., Scholze, P., Sakamoto, S., Hamachi, I., Di Giovanni, G., Chagraoui, A., 2023b. Coronaridine congeners induce sedative and anxiolytic-like activity in naive and stressed/anxious mice by allosteric mechanisms involving increased GABA(A) receptor affinity for GABA. Eur. J. Pharmacol. 953, 175854 https://doi.org/10.1016/j.ejphar.2023.175854.

Arias, H.R., Do Rego, J.L., Do Rego, J.C., Chen, Z., Anouar, Y., Scholze, P., Gonzales, E.B., Huang, R., Chagraoui, A., 2020a. Coronaridine congeners potentiate GABA(A) receptors and induce sedative activity in mice in a benzodiazepine-insensitive manner. Prog. Neuro-Psychopharmacol. Biol. Psychiatry 101, 109930. https://doi.org/10.1016/j.pnpbp.2020.109930.

Arias, H.R., Tae, H.S., Micheli, L., Yousuf, A., Ghelardini, C., Adams, D.J., Di Cesare Mannelli, L., 2020b. Coronaridine congeners decrease neuropathic pain in mice and inhibit alpha9alpha10 nicotinic acetylcholine receptors and Ca(V)2.2 channels. Neuropharmacology 175, 108194. https://doi.org/10.1016/j.neuropharm.2020.108194.

Besedovsky, L., Cordi, M., Wisslicen, L., Martinez-Albert, E., Born, J., Rasch, B., 2022. Hypnotic enhancement of slow-wave sleep increases sleep-associated hormone secretion and reduces sympathetic predominance in healthy humans. Commun. Biol. 5, 747. https://doi.org/10.1038/s42003-022-03643-y.

Bose, A., Tsai, J., Li, D., 2012. Early non-response in patients with severe depression: escitalopram up-titration versus switch to duloxetine. Clin. Drug Invest. 32, 373–385. https://doi.org/10.2165/11631890-000000000-00000.

Cameron, L.P., Patel, S.D., Vargas, M.V., Barragan, E.V., Saeger, H.N., Warren, H.T., Chow, W.L., Gray, J.A., Olson, D.E., 2023. 5-HT2ARs mediate therapeutic behavioral effects of psychedelic Tryptamines. ACS Chem. Neurosci. 14, 351–358. https://doi.org/10.1021/acschemneuro.2c00718.

Cameron, L.P., Tombari, R.J., Lu, J., Pell, A.J., Hurley, Z.Q., Ehinger, Y., Vargas, M.V., McCarroll, M.N., Taylor, J.C., Myers-Turnbull, D., Liu, T., Yaghoobi, B., Laskowski, L.J., Anderson, E.I., Zhang, G., Viswanathan, J., Brown, B.M., Tjia, M., Dunlap, L.E., Rabow, Z.T., Fiehn, O., Wulff, H., McCorvy, J.D., Lein, P.J., Kokel, D., Ron, D., Peters, J., Zuo, Y., Olson, D.E., 2021. A non-hallucinogenic psychedelic analogue with therapeutic potential. Nature 589, 474–479. https://doi.org/10.1038/s41586-020-3008-z.

Cao, C., Barros-Alvarez, X., Zhang, S., Kim, K., Damgen, M.A., Panova, O., Suomivuori, C. M., Fay, J.F., Zhong, X., Krumm, B.E., Gumpper, R.H., Seven, A.B., Robertson, M.J., Krogan, N.J., Huttenhain, R., Nichols, D.E., Dror, R.O., Skiniotis, G., Roth, B.L., 2022a. Signaling snapshots of a serotonin receptor activated by the prototypical psychedelic LSD. Neuron 110, 3154–3167. https://doi.org/10.1016/j.neuron.2022.08.006 e3157.

Cao, D., Yu, J., Wang, H., Luo, Z., Liu, X., He, L., Qi, J., Fan, L., Tang, L., Chen, Z., Li, J., Cheng, J., Wang, S., 2022b. Structure-based discovery of nonhallucinogenic psychedelic analogs. Science 375, 403–411. https://doi.org/10.1126/science.abl8615.

Carhart-Harris, R., Giribaldi, B., Watts, R., Baker-Jones, M., Murphy-Beiner, A., Murphy, R., Martell, J., Blemings, A., Erritzoe, D., Nutt, D.J., 2021. Trial of psilocybin versus escitalopram for depression. N. Engl. J. Med. 384, 1402–1411. https://doi.org/10.1056/NEJMoa2032994.

Case, D., Ben-Shalom, I., Brozell, S., Cerutti, D., Cheatham, T., Cruzeiro III, V., Darden, T., Duke, R., Ghoreishi, D., Giambasu, G., 2019. Amber, vol. 2019. University of California, San Francisco.

Casey, A.B., Mukherjee, M., McGlynn, R.P., Cui, M., Kohut, S.J., Booth, R.G., 2022. A new class of 5-HT(2A)/5-HT(2C) receptor inverse agonists: Synthesis, molecular modeling, in vitro and in vivo pharmacology of novel 2-aminotetralins. Br. J. Pharmacol. 179, 2610–2630. https://doi.org/10.1111/bph.15756.

Cheng, Y., Prusoff, W.H., 1973. Relationship between the inhibition constant (K1) and the concentration of inhibitor which causes 50 per cent inhibition (I50) of an enzymatic reaction. Biochem. Pharmacol. 22, 3099–3108. https://doi.org/10.1016/0006-2952(73)90196-2.

Contreras, A., Khumnark, M., Hines, R.M., Hines, D.J., 2021. Behavioral arrest and a characteristic slow waveform are hallmark responses to selective 5-HT(2A) receptor activation. Sci. Rep. 11, 1925. https://doi.org/10.1038/s41598-021-81552-6.

Cumming, P., Scheidegger, M., Dornbierer, D., Palner, M., Quednow, B.B., Martin-Soelch, C., 2021. Molecular and functional imaging studies of psychedelic drug action in animals and humans. Molecules 26. https://doi.org/10.3390/molecules26092451.

Diez-Alarcia, R., Muguruza, C., Rivero, G., Garcia-Bea, A., Gomez-Vallejo, V., Callado, L. F., Llop, J., Martin, A., Meana, J.J., 2021. Opposite alterations of 5-HT(2A) receptor brain density in subjects with schizophrenia: relevance of radiotracers pharmacological profile. Transl. Psychiatry 11, 302. https://doi.org/10.1038/s41398-021-01430-7.

DiMaio, F., Zhang, J., Chiu, W., Baker, D., 2013. Cryo-EM model validation using independent map reconstructions. Protein Sci. 22, 865–868. https://doi.org/10.1002/pro.2267.

Dos Santos, R.G., Hallak, J.E., Baker, G., Dursun, S., 2021. Hallucinogenic/psychedelic 5HT2A receptor agonists as rapid antidepressant therapeutics: evidence and mechanisms of action. J. Psychopharmacol. 35, 453–458. https://doi.org/10.1177/0269881120986422.

Fantegrossi, W.E., Simoneau, J., Cohen, M.S., Zimmerman, S.M., Henson, C.M., Rice, K. C., Woods, J.H., 2010. Interaction of 5-HT2A and 5-HT2C receptors in R(-)-2,5-dimethoxy-4-iodoamphetamine-elicited head twitch behavior in mice. J. Pharmacol. Exp. Therapeut. 335, 728–734. https://doi.org/10.1124/jpet.110.172247.

Fox, M.A., French, H.T., LaPorte, J.L., Blackler, A.R., Murphy, D.L., 2010. The serotonin 5-HT(2A) receptor agonist TCB-2: a behavioral and neurophysiological analysis. Psychopharmacology (Berl) 212, 13–23. https://doi.org/10.1007/s00213-009-1694-1.

Gonzalez-Maeso, J., Weisstaub, N.V., Zhou, M., Chan, P., Ivic, L., Ang, R., Lira, A., Bradley-Moore, M., Ge, Y., Zhou, Q., Sealfon, S.C., Gingrich, J.A., 2007. Hallucinogens recruit specific cortical 5-HT(2A) receptor-mediated signaling pathways to affect behavior. Neuron 53, 439–452. https://doi.org/10.1016/j.neuron.2007.01.008.

Greene, R.W., Frank, M.G., 2010. Slow wave activity during sleep: functional and therapeutic implications. Neuroscientist 16, 618–633. https://doi.org/10.1177/1073858410377064.

Halberstadt, A.L., 2015. Recent advances in the neuropsychopharmacology of serotonergic hallucinogens. Behav. Brain Res. 277, 99–120. https://doi.org/10.1016/j.bbr.2014.07.016.

He, X., Man, V.H., Yang, W., Lee, T.S., Wang, J., 2020. A fast and high-quality charge model for the next generation general AMBER force field. J. Chem. Phys. 153, 114502 https://doi.org/10.1063/5.0019056.

Heinsbroek, J.A., Giannotti, G., Bonilla, J., Olson, D.E., Peters, J., 2023. Tabernanthalog reduces Motivation for Heroin and Alcohol in a Polydrug Use model. Psychedelic Med (New Rochelle) 1, 111–119. https://doi.org/10.1089/psymed.2023.0009.

Hicks, J.K., Bishop, J.R., Sangkuhl, K., Muller, D.J., Ji, Y., Leckband, S.G., Leeder, J.S., Graham, R.L., Chiulli, D.L., A, L.L., Skaar, T.C., Scott, S.A., Stingl, J.C., Klein, T.E., Caudle, K.E., Gaedigk, A., Clinical Pharmacogenetics Implementation, C., 2015. Clinical Pharmacogenetics Implementation Consortium (CPIC) guideline for CYP2D6 and CYP2C19 genotypes and dosing of selective serotonin reuptake inhibitors. Clin. Pharmacol. Ther. 98, 127–134. https://doi.org/10.1002/cpt.147.

Hines, R.M., Aquino, E.A., Khumnark, M.I., Davila, M.P., Hines, D.J., 2022. Comparative assessment of TSPO modulators on electroencephalogram activity and exploratory behavior. Front. Pharmacol. 13, 750554 https://doi.org/10.3389/fphar.2022.750554.

Hines, R.M., Maric, H.M., Hines, D.J., Modgil, A., Panzanelli, P., Nakamura, Y., Nathanson, A.J., Cross, A., Deeb, T., Brandon, N.J., Davies, P., Fritschy, J.M., Schindelin, H., Moss, S.J., 2018. Developmental seizures and mortality result from reducing GABA(A) receptor alpha2-subunit interaction with collybistin. Nat. Commun. 9, 3130. https://doi.org/10.1038/s41467-018-05481-1.

Holze, F., Gasser, P., Muller, F., Dolder, P.C., Liechti, M.E., 2023. Lysergic acid diethylamide-assisted therapy in patients with anxiety with and without a life-threatening illness: a randomized, double-blind, placebo-controlled phase II study. Biol. Psychiatr. 93, 215–223. https://doi.org/10.1016/j.biopsych.2022.08.025.

Holze, F., Vizeli, P., Muller, F., Ley, L., Duerig, R., Varghese, N., Eckert, A., Borgwardt, S., Liechti, M.E., 2020. Distinct acute effects of LSD, MDMA, and D-amphetamine in healthy subjects. Neuropsychopharmacology 45, 462–471. https://doi.org/10.1038/s41386-019-0569-3.

Izadi, S., Onufriev, A.V., 2016. Accuracy limit of rigid 3-point water models. J. Chem. Phys. 145, 074501 https://doi.org/10.1063/1.4960175.

Jakalian, A., Jack, D.B., Bayly, C.I., 2002. Fast, efficient generation of high-quality atomic charges. AM1-BCC model: II. Parameterization and validation. J. Comput. Chem. 23, 1623–1641. https://doi.org/10.1002/jcc.10128.

Jaster, A.M., Elder, H., Marsh, S.A., de la Fuente Revenga, M., Negus, S.S., Gonzalez-Maeso, J., 2022. Effects of the 5-HT(2A) receptor antagonist volinanserin on head-twitch response and intracranial self-stimulation depression induced by different structural classes of psychedelics in rodents. Psychopharmacology (Berl) 239, 1665–1677. https://doi.org/10.1007/s00213-022-06092-x.

Klemm, W.R., 2001. Behavioral arrest: in search of the neural control system. Prog. Neurobiol. 65, 453–471. https://doi.org/10.1016/s0301-0082(01)00016-8.

Kurrasch-Orbaugh, D.M., Watts, V.J., Barker, E.L., Nichols, D.E., 2003. Serotonin 5-hydroxytryptamine 2A receptor-coupled phospholipase C and phospholipase A2 signaling pathways have different receptor reserves. J. Pharmacol. Exp. Therapeut. 304, 229–237. https://doi.org/10.1124/jpet.102.042184.

Leger, D., Debellemaniere, E., Rabat, A., Bayon, V., Benchenane, K., Chennaoui, M., 2018. Slow-wave sleep: from the cell to the clinic. Sleep Med. Rev. 41, 113–132. https://doi.org/10.1016/j.smrv.2018.01.008.

Liu, X., Zhu, H., Gao, H., Tian, X., Tan, B., Su, R., 2022. G(s) signaling pathway distinguishes hallucinogenic and nonhallucinogenic 5-HT(2A)R agonists induced head twitch response in mice. Biochem. Biophys. Res. Commun. 598, 20–25. https://doi.org/10.1016/j.bbrc.2022.01.113.

Lomize, M.A., Pogozheva, I.D., Joo, H., Mosberg, H.I., Lomize, A.L., 2012. OPM database and PPM web server: resources for positioning of proteins in membranes. Nucleic Acids Res. 40, D370–D376. https://doi.org/10.1177/10.1093/nar/gkr703.

Lopez-Gimenez, J.F., Gonzalez-Maeso, J., 2018. Hallucinogens and serotonin 5-HT(2A) receptor-mediated signaling pathways. Curr Top Behav Neurosci 36, 45–73. https://doi.org/10.1007/7854_2017_478.

Lu, J., Tjia, M., Mullen, B., Cao, B., Lukasiewicz, K., Shah-Morales, S., Weiser, S., Cameron, L.P., Olson, D.E., Chen, L., Zuo, Y., 2021. An analog of psychedelics restores functional neural circuits disrupted by unpredictable stress. Mol. Psychiatr. 26, 6237–6252. https://doi.org/10.1038/s41380-021-01159-1.

Luethi, D., Trachsel, D., Hoener, M.C., Liechti, M.E., 2018. Monoamine receptor interaction profiles of 4-thio-substituted phenethylamines (2C-T drugs). Neuropharmacology 134, 141–148. https://doi.org/10.1016/j.neuropharm.2017.07.012.

Luz, M., Mash, D.C., 2021. Evaluating the toxicity and therapeutic potential of ibogaine in the treatment of chronic opioid abuse. Expet Opin. Drug Metabol. Toxicol. 17, 1019–1022. https://doi.org/10.1080/17425255.2021.1944099.

Meiler, J., Baker, D., 2006. ROSETTALIGAND: protein-small molecule docking with full side-chain flexibility. Proteins 65, 538–548. https://doi.org/10.1002/prot.21086.

Mendenhall, J., Brown, B.P., Kothiwale, S., Meiler, J., 2021. BCL::Conf: improved open-source knowledge-based conformation sampling using the crystallography open database. J. Chem. Inf. Model. 61, 189–201. https://doi.org/10.1021/acs.jcim.0c01140.

Moreno, J.L., Holloway, T., Albizu, L., Sealfon, S.C., Gonzalez-Maeso, J., 2011. Metabotropic glutamate mGlu2 receptor is necessary for the pharmacological and behavioral effects induced by hallucinogenic 5-HT2A receptor agonists. Neurosci. Lett. 493, 76–79. https://doi.org/10.1016/j.neulet.2011.01.046.

Moya, P.R., Berg, K.A., Gutierrez-Hernandez, M.A., Saez-Briones, P., Reyes-Parada, M., Cassels, B.K., Clarke, W.P., 2007. Functional selectivity of hallucinogenic phenethylamine and phenylisopropylamine derivatives at human 5-hydroxytryptamine (5-HT)2A and 5-HT2C receptors. J. Pharmacol. Exp. Therapeut. 321, 1054–1061. https://doi.org/10.1124/jpet.106.117507.

Muguruza, C., Miranda-Azpiazu, P., Diez-Alarcia, R., Morentin, B., Gonzalez-Maeso, J., Callado, L.F., Meana, J.J., 2014. Evaluation of 5-HT2A and mGlu2/3 receptors in postmortem prefrontal cortex of subjects with major depressive disorder: effect of antidepressant treatment. Neuropharmacology 86, 311–318. https://doi.org/10.1016/j.neuropharm.2014.08.009.

Muneta-Arrate, I., Diez-Alarcia, R., Horrillo, I., Meana, J.J., 2020. Pimavanserin exhibits serotonin 5-HT(2A) receptor inverse agonism for G(alphai1)- and neutral antagonism for G(alphaq/11)-proteins in human brain cortex. Eur. Neuropsychopharmacol 36, 83–89. https://doi.org/10.1016/j.euroneuro.2020.05.004.

Nichols, D.E., 2004. Hallucinogens. Pharmacol. Ther. 101, 131–181. https://doi.org/10.1016/j.pharmthera.2003.11.002.

Oathes, D.J., Ray, W.J., Yamasaki, A.S., Borkovec, T.D., Castonguay, L.G., Newman, M. G., Nitschke, J., 2008. Worry, generalized anxiety disorder, and emotion: evidence from the EEG gamma band. Biol. Psychol. 79, 165–170. https://doi.org/10.1016/j.biopsycho.2008.04.005.

Pallavicini, C., Vilas, M.G., Villarreal, M., Zamberlan, F., Muthukumaraswamy, S., Nutt, D., Carhart-Harris, R., Tagliazucchi, E., 2019. Spectral signatures of serotonergic psychedelics and glutamatergic dissociatives. Neuroimage 200, 281–291. https://doi.org/10.1016/j.neuroimage.2019.06.053.

Pedzich, B.D., Rubens, S., Sekssaoui, M., Pierre, A., Van Schuerbeek, A., Marin, P., Bockaert, J., Valjent, E., Becamel, C., De Bundel, D., 2022. Effects of a psychedelic 5-HT2A receptor agonist on anxiety-related behavior and fear processing in mice. Neuropsychopharmacology 47, 1304–1314. https://doi.org/10.1038/s41386-022-01324-2.

Rodriguez, P., Urbanavicius, J., Prieto, J.P., Fabius, S., Reyes, A.L., Havel, V., Sames, D., Scorza, C., Carrera, I., 2020. A single administration of the atypical psychedelic ibogaine or its metabolite noribogaine induces an antidepressant-like effect in rats. ACS Chem. Neurosci. 11, 1661–1672. https://doi.org/10.1021/acschemneuro.0c00152.

Roe, D.R., Cheatham 3rd, T.E., 2013. PTRAJ and CPPTRAJ: software for processing and analysis of molecular dynamics trajectory data. J. Chem. Theor. Comput. 9, 3084–3095. https://doi.org/10.1021/ct400341p.

Serafine, K.M., Rice, K.C., France, C.P., 2015. Directly observable behavioral effects of lorcaserin in rats. J. Pharmacol. Exp. Therapeut. 355, 381–385. https://doi.org/10.1124/jpet.115.228148.

Sherin, J.E., Nemeroff, C.B., 2011. Post-traumatic stress disorder: the neurobiological impact of psychological trauma. Dialogues Clin. Neurosci. 13, 263–278. https://doi.org/10.31887/DCNS.2011.13.2/jsherin.

Tae, H.S., Ortells, M.O., Tekarli, B.J., Manetti, D., Romanelli, M.N., McIntosh, J.M., Adams, D.J., Arias, H.R., 2023. DM506 (3-Methyl-1,2,3,4,5,6-hexahydroazepino [4,5-b]indole fumarate), a novel derivative of ibogamine, inhibits alpha7 and alpha9alpha10 nicotinic acetylcholine receptors by different allosteric mechanisms. ACS Chem. Neurosci. 14, 2537–2547. https://doi.org/10.1021/acschemneuro.3c00212.

Tian, C., Kasavajhala, K., Belfon, K.A.A., Raguette, L., Huang, H., Migues, A.N., Bickel, J., Wang, Y., Pincay, J., Wu, Q., Simmerling, C., 2020. ff19SB: amino-acid-specific protein backbone parameters trained against quantum mechanics energy surfaces in solution. J. Chem. Theor. Comput. 16, 528–552. https://doi.org/10.1021/acs.jctc.9b00591.

Vahid-Ansari, F., Zhang, M., Zahrai, A., Albert, P.R., 2019. Overcoming resistance to selective serotonin reuptake inhibitors: targeting serotonin, serotonin-1A receptors and adult neuroplasticity. Front. Neurosci. 13, 404. https://doi.org/10.3389/fnins.2019.00404.

Vollenweider, F.X., Kometer, M., 2010. The neurobiology of psychedelic drugs: implications for the treatment of mood disorders. Nat. Rev. Neurosci. 11, 642–651. https://doi.org/10.1038/nrn2884.

Weber, E.T., Andrade, R., 2010. Htr2a gene and 5-ht2a receptor expression in the cerebral cortex studied using genetically modified mice. Front. Neurosci. https://doi.org/10.3389/fnins.2010.00036.

Wu, E.L., Cheng, X., Jo, S., Rui, H., Song, K.C., Davila-Contreras, E.M., Qi, Y., Lee, J., Monje-Galvan, V., Venable, R.M., Klauda, J.B., Im, W., 2014. CHARMM-GUI Membrane Builder toward realistic biological membrane simulations. J. Comput. Chem. 35, 1997–2004. https://doi.org/10.1002/jcc.23702.